Numerical simulations of the intensity change of Typhoon Choiwan (2009) and the oceanic response

Akiyoshi Wada
*Meteorological Research Institute, Tsukuba, Ibaraki, 305-0052, JAPAN
awada@mri-jma.go.jp

1. Introduction

Interactions between typhoons and the ocean are known to be important for predicting their intensity changes. In addition, a strong wind curl accompanied by typhoons induces sea surface cooling by passage of a TC, and causes variations in $p\mathrm{CO}_2$ in the upper ocean. The concentration of $p\mathrm{CO}_2$ is a function of the concentration of hydrogen ions, which is calculated by given water temperature, salinity, dissolved inorganic carbon (DIC) and total alkalinity (ALK). Wada et al. (2011a, b) reported that a simple chemical scheme coupled with an ocean general circulation model (Wada et al., 2011a) or coupled with a nonhydrostatic atmosphere model coupled with a multilayer ocean model and the third generation ocean wave model enabled us to simulate variations in $p\mathrm{CO}_2$ and air-sea CO_2 flux caused by Typhoons Tina and Winnie (1997) and Typhoon Hai-Tang (2005). However, the variations in $p\mathrm{CO}_2$ could not be validated for numerical simulations of Typhoon Hai-Tang (2005) due to lack of observation.

Bond et al. (2011) reported that $\Delta p\mathrm{CO}_2$, the water minus air value, increased dramatically giving a maximum value of 55 μatm and then it slowly decreases at the surface mooring buoy named the Kuroshio Extension Observatory (KEO) buoy by passage of Typhoon Choiwan in 2009. In order to clarify the mechanism of the variations in $p\mathrm{CO}_2$ in the upper ocean by passage of Choiwan, numerical simulations were performed using a nonhydrostatic atmosphere model coupled with the multilayer ocean model and the third generation ocean wave model.

2. Experiment design

The specification of numerical simulations performed by a nonhydrostatic atmosphere model coupled with the multilayer ocean model, the ocean wave model and the simple chemical scheme is given in this section. The computational domain is 3240 km x 3960 km with a horizontal grid spacing of 6 km. The model has 40 vertical levels with variable intervals from 40 m for the lowermost (near-surface) layer to 1180 m for the uppermost layer. The model has maximum height approaching nearly 23 km. The time step of the nonhydrostatic model is 15 s. The length of the time step of the ocean model is six times that of the atmosphere model. The initial depth of the mixed layer is determined from oceanic reanalysis data, calculated using the MRI ocean variational estimation (MOVE) system (Usui et al., 2006), by assuming a difference in the value of density from the surface of no more than 0.25 kg m^{-3} and the depth of the mixed layer is limited to 200 m. The base of the thermocline is limited to 600 m and water depth is limited to 2000 m.

Table 1 shows a list of numerical experiments. Acronyms are the same as Wada (2012), which is determined from the model whether noncoupled atmosphere or coupled atmosphere-ocean model, their horizontal resolution, the type of atmospheric initial and lateral boundary condition ("G" means global analysis data made in Japan Meteorological Agency), horizontal resolution of oceanic reanalysis data, and cloud physics ("I" means inclusion of ice phase).

Table 1 A list of numerical simulations

	Coupled ocean / Noncoupled	Horizontal resolution of oceanic reanalysis data
A6G5I	Noncoupled	0.5
A6G1I	Noncoupled	0.1
C6G5I	Coupled	0.5
C6G1I	Coupled	0.1

The integration hour is 96 hours. The lateral boundary condition is changed every six hours. The momentum, sensible and latent heat fluxes are given to the ocean model. It should be noted that the normalization of DIC and ALK to a salinity of 34.1 from a salinity of 35.0 was done at the initial time of numerical simulations. In addition, ALK at the initial time are determined from the following formula.

$$ALK_{init} = \begin{cases} 2500.9T_i^{-0.0029} & T > 18.0 \\ 2299.818 & T \leq 18.0 \end{cases}, \qquad (1)$$

where T_i is water temperature at the i-th level of the multilayer ocean model. DIC at the initial time are determined from the formula as described in Wada et al. (2011a).

3. Results

Figure 1 compares the results of track simulations (close diamonds in A6G1I, close triangles in C6G1I, open diamonds in A6G5I and open triangles in C6G5I) with the best track (gray circles) archived in the Japan Meteorological Agency. The tracks simulated by the model agree well to the best track although the translation speed of simulated typhoons tends to be slow. A westward bias reported in Wada (2012) reduces due to a change of the width of lateral boundary relaxation sponge layers from 20 to 70.

Time series of simulated central pressures indicates that the coupled model leads to an increase in simulated central pressure after 24 h (Figure 2), corresponding to the end of the intensification except in A6G1I. Also, the central pressure in C6G5I is higher than that in C6G1I, indicating that an oceanic initial environmental field plays a crucial role in the intensity simulation of Typhoon Choi-wan.

A horizontal distribution of precipitation by SSMIS satellite microwave sensor has an asymmetric wave-number 1 pattern, implying that this typhoon changes to an occlusive cyclone (Figure 3a). The model well simulated the wave-number 1 precipitation pattern in C6G5I (Figure 3b) and C6G1I (Figure 3c). The amount of precipitation, particularly around 33°N, 143°E in C6G1I is higher than that in C6G5I. This suggests that an oceanic environmental field can affect the amount of the precipitation even around the eyewall and spiral-band region.

Time series of sea surface temperature (SST) in C6G5I (Figure 4a) and C6G1I (Figure 4b) indicate that SST decreases by nearly 2.5ºC around the KEO buoy during the integration, which is greater than that of Bond et al. (2011). The time series of $p\mathrm{CO_2}$ in C6G5I (Figure 4c) and C6G1I (Figure 4d) show that $p\mathrm{CO_2}$ gradually increases and then decreases after 72 h. Even though these simulations assume that $p\mathrm{CO_2}$ in the atmosphere is a constant during the integration, these simulations poorly reproduce a "dramatically" increase in $p\mathrm{CO_2}$ in the upper ocean. Bond et al. (2011) showed that a rapid decrease in SST (corresponding to 48 h integration time) started at 1200 UTC 19 September when the sea-level pressure suddenly decreased and $\Delta\mathrm{CO_2}$ rapidly increased. However, simulated SST started at 63 h, 15 h later than the result of Bond et al. (2011). The accuracy of track prediction of the typhoon, including the translation speed may be important for the variation of $\Delta\mathrm{CO_2}$.

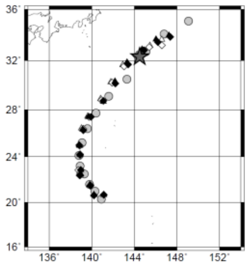

Figure 1 Best track of Choi-wan and results of track simulations from the initial time to 84h

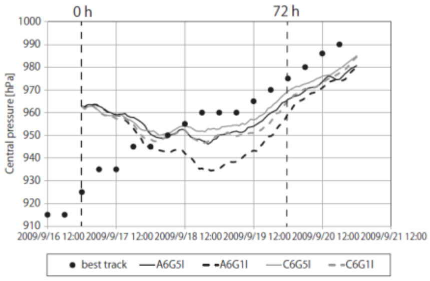

Figure 2 Best-track central pressure of Choi-wan and results of central pressure simulations from the initial time to 96h.

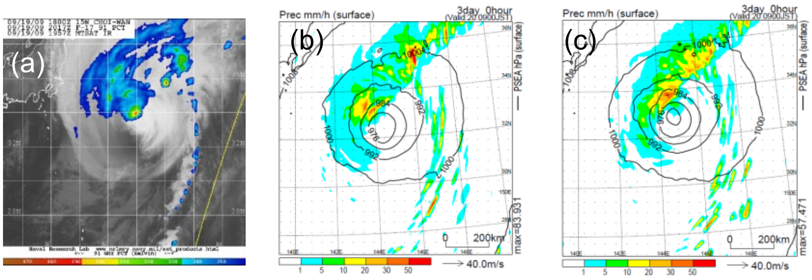

Figure 3 Horizontal distribution of precipitation (a) by SSMIS satellite microwave sensor, (b) that at 72 h in C6G5I, and (c) that at 72 h in C6G1I.

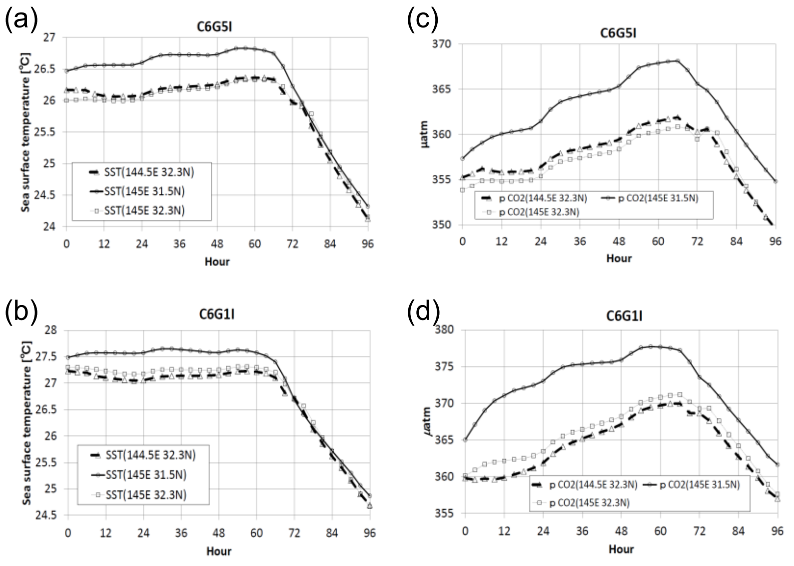

Figure 4 Time series of (a) SST in C6G5I, (b) SST in C6G1I, (c) PCO2 at the surface in C6G5I and (d) PCO2 at the surface in C6G1I around the KEO moored buoy.

4. Discussion and conclusion

This study suggests that an oceanic environmental field also affects the variation of $p\mathrm{CO_2}$ in the upper ocean in addition to the effect of the translation speed of the typhoon on the variation of $p\mathrm{CO_2}$ in the upper ocean. In fact, simulated SST in C6G5I is lower than that in C6G1I, resulting in low value of $p\mathrm{CO_2}$ in the upper ocean.

Because of poor vertical resolution and simplified physics of the multilayer ocean model, the effect of background currents on the variation of $p\mathrm{CO_2}$ in the upper ocean could not be simulated in this study. In order to investigate this issue, a sophisticated ocean general circulation model will be needed. The numerical simulations of Typhoon Choi-wan seem to be reasonable in that the track simulations agree to the best track. However, they are insufficient to reproduce the variation of SST and $p\mathrm{CO_2}$ observed at the KEO buoy. We need to explore much more accuracy for the simulations.

Acknowledgement

This work was supported by the Japan Society for the Promotion of Science (JSPS), Grant-in-Aid for Scientific Research (C) (22540454) and on Innovative Areas (Research in a proposed research area) (23106505).

References

Bond, N. A., M. F. Cronin, C. Sabine, Y. Kawai, H. Ichikawa, P. Freitag, and K. Ronnholm (2011), Upper ocean response to Typhoon Choi-wan as measured by the Kuroshio Extension Observatory mooring, *J. Geophys., Res*., 116, C02031.

Usui, N., Ishizaki S., Fujii Y., Tsujino H., Yasuda T., and Kamachi M. (2006), Meteorological Research Institute multivariate ocean variational estimation (MOVE) system: Some early results. *Advances in Space Research*, **37**, 896-822.

Wada, A., 2012: *Numerical study on the effect of the ocean on tropical-cyclone intensity and structural change*, Atmospheric Models. (Ed. I. Yucel) InTech, in press.

Wada, A., T. Midorikawa, M. Ishii, and T. Motoi (2011a), Carbon system changes in the East China Sea induced by Typhoons Tina and Winnie in 1997, *J. Geophys. Res.*, **116**, C07014.

Wada, A., T. Midorikawa and M. Ishii (2011b), Variations in air-sea CO2 flux and PH induced by passage of typhoon Hai-Tang (2005), *CAS/JSC WGNE Res. Activ. Atmos. Oceanic. Modell.* **41**, 9-11